ELSEVIER

Int. J. Therm. Sci. 41 (2002) 528–535

International Journal of Thermal Sciences

www.elsevier.com/locate/ijts

An inverse heat transfer problem for restoring the temperature field in a polymer melt flow through a narrow channel ☆

Igor Gejadze [a], Yvon Jarny [b]

[a] *Department of Applied Math. and Computer Science, The Weizmann Institute of Science, 76100 Rehovot, Israel*
[b] *Laboratoire de Thermocinetique, UMR CNRS 6607, Ecole Polytechnique de l'Université de Nantes, BP 50609, 44306 Nantes cedex 3, France*

Received 4 October 2001; accepted 20 March 2002

Abstract

An important problem in polymer processing is to provide suitable thermal conditions for polymer melt flows through narrow channels during extrusion or injection. Due to various thermal effects (e.g., viscous dissipation, chemical reactions) the temperature profile of the melt could be quite sharp. In order to numerically simulate polymer flows and heat transfer through a narrow channel, the inlet boundary conditions, which are generally unknown, have to be specified. For such a creeping flow, the area where the velocity field develops is very short. In contrast, the inlet temperature profile develops quite slowly and affects the temperature field far downstream. An approach is suggested for restoring the inlet temperature profile by solving an inverse heat transfer problem using Cauchy data at the channel wall. The polymer flow is assumed to be a steady, laminar and incompressible flow of a non-Newtonian pseudo-plastic fluid, which is governed by the Navier–Stokes equations and a constitutive "power law" model for viscosity. This non-linear inverse problem is solved by a sequential approximation method combined with Tikhonov's regularization method. Notably, this approach has been found to be efficient for field observation problems, when the magnitude of non-linearity is not too large. The results of numerical simulation are presented and questions regarding accuracy are discussed.

Keywords: Inverse heat transfer; Polymer processing; Temperature profile restoration

1. Introduction

Numerical and experimental investigations of polymer flows and the corresponding heat transfer problems constitute an important part of research on polymer (food) extrusion and injection. Some studies, based on the numerical solution of the equations governing flow and heat transfer in two and three dimensions, were recently carried out by Lin and Jaluria [1,2], Hammad and Vradis [3], and others. Commercial software (e.g., POLYFLOW, FIDAP and MOLDFLOW) enable considering the flow of polymer melts for different complex geometries and viscosity models. However, in order to obtain accurate numerical solutions, inlet boundary conditions must be carefully specified. For example, in modeling polymer melt flows through a die, researches usually consider the die as a stand alone tool, independent of the extrusion conditions that feed the melt into the die. The initial velocity profile is usually assumed to be fully developed. This approach becomes limited if the screws feeding the die are situated close to the die entrance. Concerning the inlet temperature profile, two main characteristics of the polymer melt flow have to be taken into account: (a) due to the very high Peclet number, the inlet profile affects the viscosity field in the die at a distance far from the entrance, (b) due to high viscous dissipation and very low heat conductivity, the temperature profile could have a sharp form and the maximum temperature in the flow approaches the die wall where the fluid has a high residence time. As a result, an overheated area can be generated within the flow and degradation of material could occur. Therefore, it is important to accurately predict and control the maximum temperature rise within the polymer melt flow.

The question considered in this study concerns the feasibility of restoring the temperature field within the fluid, by taking the temperature measured at the channel wall and possibly in some additional locations within the flow, when the inlet profile is unknown. This problem belongs to the

☆ This article is a follow up a communication presented by the authors at the EUROTHERM Seminar 68, "Inverse problems and experimental design in thermal and mechanical engineering", held in Poitiers in March 2001.

E-mail address: yvon.jarny@polytech.univ-nantes.fr (Y. Jarny).

1290-0729/02/$ – see front matter
PII: S1290-0729(02)01346-7

Nomenclature

c	specific heat capacity	$\mathrm{J\cdot kg^{-1}\cdot K^{-1}}$
Ec	Eckert number $= u_{\mathrm{ref}}^2 c_{\mathrm{ref}}^{-1} T_{\mathrm{ref}}^{-1}$	
L	channel length	m
m	number of iterations	
p	local pressure	Pa
Pe	Peclet number $= [u\rho c R\cdot \lambda^{-1}]_{\mathrm{ref}}$	
R	inlet channel radius	m
$R(x)$	channel boundary shape	
r	radial coordinate	m
Re	Reynolds number $= [uR\rho/\eta]_{\mathrm{ref}}$	
T	temperature	K
u	axial velocity component	$\mathrm{m\cdot s^{-1}}$
v	radial velocity component	$\mathrm{m\cdot s^{-1}}$
x	axial coordinate	m

Greek letters

α	regularization parameter, Eq. (26)	
β	temperature coefficient of viscosity, Eq. (8)	$\mathrm{K^{-1}}$
χ	the residual level	
$\dot{\gamma}$	shear rate	$\mathrm{s^{-1}}$
Φ	viscous dissipation function	
λ	thermal conductivity	$\mathrm{W\cdot m^{-1}\cdot K^{-1}}$
ν	"power law" index, Eq. (8)	
ρ	density	$\mathrm{kg\cdot m^{-3}}$
η	viscosity	Pa·s

Subscripts/Superscripts

u_x	derivative $= \partial u/\partial x$
u_r	derivative $= \partial u/\partial r$
$u_{\vec{n}}$	normal derivative $= du/d\vec{n}$
ref	reference value
in	inlet value
r'	new r variable
$\widehat{\ }$	measured values

inverse heat transfer problems (IHTP) group. They were systematically considered by Alifanov [4] and others. The basic equation governing the phenomenon is the convection–diffusion equation. IHTP generally consists in determining the temperature field within a given spatial domain (field observation problem) or in the estimation of coefficients (identification problem), assuming that additional noisy measurement data (temperatures and/or heat fluxes) are available. The aim of the problem under investigation is to restore the inlet temperature profile using the Cauchy data measured at the channel wall.

When the coefficients of the convection–diffusion equation are known, i.e. the velocity field, a unique IHTP solution can be expected. If the velocity field does not depend on the temperature field, the IHTP solution is simplified, in a recent study, Huang and Chen [5] considered this situation for non-stationary Navier–Stokes (N–S) equations. For natural convection flows, the buoyancy force depends on temperature. A natural convection IHTP solution was studied by Prud'homme and Nguyen [6]. Obviously when the viscosity strongly depends on temperature, coupling between the temperature and the velocity fields is essential for fluid flows through narrow channels.

In this paper, we studied the coupled IHTP, where the velocity field depends on the temperature field through viscosity, using generalized N–S equations for a non-Newtonian fluid. We show that under the usual polymer processing conditions, such a coupling has to be taken into account for polymer melt flows though narrow channels like extrusion or injection die. In conclusion, the IHTP methodology is suggested to improve the prediction of thermal effects in polymer flows.

2. Direct problem statement

An arbitrary boundary-shaped cylindrical channel is considered in Fig. 1. The dimensionless equations that govern the steady, laminar, and incompressible flow of a non-Newtonian fluid (polymer melt) in cylindrical coordinates are [1]

$$u_x + \frac{1}{r}(rv)_r = 0 \tag{1}$$

$$vv_r + uv_x + p_r = \frac{1}{Re}\left(\frac{1}{r}(\eta r v_r)_r + (\eta v_x)_x + \eta_r v_r + \eta_x u_r - \eta\frac{v}{r^2}\right) \tag{2}$$

$$vu_r + uu_x + p_x = \frac{1}{Re}\left(\frac{1}{r}(\eta r u_r)_r + (\eta u_x)_x + \eta_r v_x + \eta_x u_x\right) \tag{3}$$

$$0 < x < L, \qquad 0 < r < R(x)$$

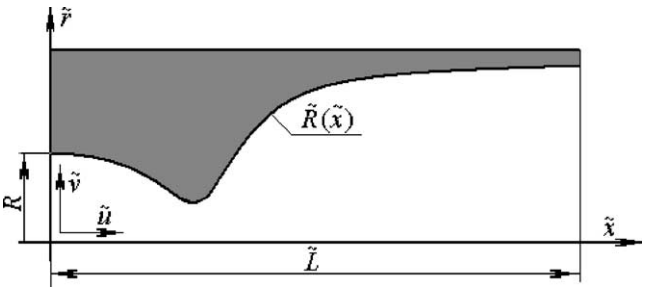

Fig. 1. Cylindrical arbitrary shaped polymer melt flow channel.

Heat transfer within the fluid is governed by the non-linear convection–diffusion (energy) equation

$$(uT_x + vT_r) = \frac{1}{Pe}\left[(T_x)_x + \frac{1}{r}(rT_r)_r\right] + \frac{Ec}{Re}\Phi \tag{4}$$

where u, v are functions of the field $T(x,r)$.

The dimensionless variables are taken as follows:

$$\begin{array}{ll} u = \tilde{u}/u_{\text{ref}}, & v = \tilde{v}/u_{\text{ref}} \\ p = \tilde{p}/\left(\rho u_{\text{ref}}^2\right), & T = \left(\widetilde{T} - T_{\text{ref}}\right)/T_{\text{ref}} \\ \eta = \tilde{\eta}/\eta_{\text{ref}}, & q_w = \tilde{q}_w R/(\lambda_{\text{ref}} T_{\text{ref}}) \\ x = \tilde{x}/R, & r = \tilde{r}/R \\ R(x) = \widetilde{R}(x)/R, & L = \widetilde{L}/R \end{array}$$

The shear rate and the dimensionless shear rate are given by the following equations

$$\tilde{\dot{\gamma}} = \frac{u_{\text{ref}}}{R}\dot{\gamma} \tag{5}$$

and

$$\dot{\gamma} = \left[2\left(u_x^2 + v_r^2 + v^2/r^2\right) + \left(u_r^2 + v_x^2\right)\right]^{1/2} \tag{6}$$

The dimensionless viscous dissipation function is given by

$$\Phi(T) = \eta\dot{\gamma}^2 \tag{7}$$

$$\tilde{\eta} = \eta\left(\widetilde{T}, \tilde{\dot{\gamma}}\left(T(x,r)\right)\right)$$

The viscosity varies mostly with respect to shear rate and temperature. In the present study the "power law" model is considered

$$\tilde{\eta} = \eta_{\text{ref}}\left(\tilde{\dot{\gamma}}\right)^{\nu-1} e^{-\beta(\widetilde{T} - T_{\text{ref}})} \tag{8}$$

where ν is called the "power law" index.

Eqs. (1)–(3) together with Eq. (8) describe the pseudo-plastic behavior of the fluid. Variations with respect to pressure or concentration of chemical species could be taken into account. Other constitutive models (see, for example, [7]) are also available.

The boundary conditions for the flow equations are specified as follows:

$$\begin{array}{lll} u_r(x,0) = 0, & v(x,0) = 0, & 0 < x < L \\ u\left(x, R(x)\right) = 0, & v\left(x, R(x)\right) = 0, & 0 < x < L \\ u(0,r) = u_{\text{in}}(r), & v(0,r) = v_{\text{in}}(r), & 0 < r < R(x) \\ u_x(L,r) = 0, & v_x(L,r) = 0, & 0 < r < R(x) \end{array} \tag{9}$$

and for the energy equation, as follows:

$$\begin{array}{ll} T_r(x,0) = 0, & 0 < x \leqslant L \\ T_x(L,r) = 0, & 0 \leqslant r \leqslant R(L) \end{array} \tag{10}$$

$$\begin{array}{ll} -T_{\vec{n}}\left(x, R(x)\right) = q_w(x), & 0 < x \leqslant L \\ T(0,r) = w(r), & 0 \leqslant r \leqslant 1 \end{array} \tag{11}$$

3. Inverse problem statement

Heat transfer in the polymer melt is governed by Eqs. (4)–(7), together with the boundary conditions of Eqs. (10), (11). The flow velocity components u, v depend on temperature through viscosity (Eq. (8)) and the generalized N–S equations (1)–(3), together with the boundary conditions of Eq. (9). The numerical solution of this set of non-linear equations can be computed only when four boundary conditions are specified: the inlet velocity profiles $u_{\text{in}}(r)$ and $v_{\text{in}}(r)$, the inlet temperature profile $w(r)$, and the wall heat flux $q_w(x)$ at the polymer-die interface.

In the following study, $u_{\text{in}}(r)$, $v_{\text{in}}(r)$, and $q_w(x)$ are assumed to be known:

- $u_{\text{in}}(r)$ could be computed as the outlet velocity profile of a fully developed flow in a straight tube, therefore $v_{\text{in}}(r) = 0$.
- $q_w(x)$ could be determined by including the die in the spatial heat transfer domain under study, and by solving the conjugate heat transfer problem in both polymer and die domains. Here for simplicity, the spatial domain is restricted to the polymer flow domain and an adiabatic condition $q_w(x) = 0$ will be considered along the interface.

The polymer inlet temperature profile $w(r)$ is unknown. After being restored, the temperature $T(x,r;w)$ at any point of the polymer flow domain $(0,L) \times (0,R(x))$ will be determined by solving the direct problem equations of Section 2.

The aim of the inverse problem under consideration is to restore the radial profile $w(r)$ from additional temperature data $Y = \{Y_k(x),\ k = 1,N\}$, here assumed without errors, available along N axial measurement lines $R_k(x)$

$$Y_k(x) = T\left(x, R_k(x)\right), \quad 0 < x < L \tag{12}$$

At least one of those lines must be the channel boundary line $R(x)$.

The boundary conditions $u_{\text{in}}(r)$, $v_{\text{in}}(r)$ and $q_w(x)$ being fixed, let A be the non-linear operator that maps the inlet profile $w(r)$ onto the temperature field $T(x,r)$ in the polymer melt flow, through the non-linear equations (1)–(11):

$$Aw = T \tag{13}$$

Let C be the linear output operator that maps the temperature field $T(x,r;w)$ to the output temperature Y

$$Y = CT \tag{14}$$

and let us denote $\widehat{Y}(x)$ the measured temperature (with inherent errors):

$$\widehat{Y} = Y + \delta_T \tag{15}$$

where $\delta_T(x)$ is an error function, assumed to be Gaussian with standard deviation σ_T.

The inverse problem can be stated by the following operator equation

$$CAw - \widehat{Y} = 0 \tag{16}$$

4. Algorithm for the IHTP solution

The IHTP under consideration is an ill-posed problem and the solution is strongly affected by noisy measurements [13]. Moreover, it should be noted that the non-linear equation (16), has to be solved using an iterative algorithm. If the solution of the N–S equations is required to update the velocity components u, v and the source term Φ, at each iteration, the numerical procedure would become very time-consuming. This is why an iterative algorithm based on the combination of a sequential approximation method together with Tikhonov's regularization has been developed as explained below.

4.1. The sequential approximation method

This algorithm was found to be efficient for field restoration problems, when the deviations of the unknown field around a known state can be considered as small [8,9].

Let $w^n(r)$ be the current approximation of the inlet temperature profile and $T^n(x,r) = Aw^n(r)$ the corresponding temperature field, solution of the modeling equations (1)–(11). Let us consider a perturbation $\delta w(r)$ to the inlet temperature. Then the temperature field variation $\delta T(x,r)$ is given by the solution of the linear equation

$$\left(u^n \delta T_x + v^n \delta T_r\right) = \frac{1}{Pe}\left[(\delta T_x)_x + \frac{1}{r}(r\delta T_r)_r\right]$$

$$\delta T(0,r) = \delta w(r), \qquad \delta T_{\bar{n}}\big(x, R(x)\big) = 0$$

assuming that u^n, v^n are taken as functions of the space coordinates (x,r), according to the current field $T^n(x,r)$.

Introduce the linear operator B^n, which maps the function $\delta w = w - w^n$ onto the field variation $\delta T = T - T^n$, then the new approximation of the temperature field

$$T = T^n + \delta T = Aw^n + B^n\left(w - w^n\right)$$

is used to rewrite the inverse problem equation (16) under the new linear form

$$CB^n w = CB^n w^n + \widehat{Y} - CAw^n \tag{17}$$

The operator B^n should not be changed within the iteration loop marked with index m below. If the initial approximation w^0 is chosen close enough to its actual value, then the operator B^n could be calculated once and for all at the beginning, for $n = 1$. The sequential approximation method for solving Eq. (17) is defined by:

$$CB^n w^{m+1} = f^m, \quad m = 1, \ldots \tag{18}$$

where

$$f^m = \begin{cases} \widehat{Y}, & m = n \\ CB^n w^m + \widehat{Y} - CAw^m, & m > n \end{cases} \tag{19}$$

and $n = m$, if the operator B is changed.

The iterative process is stopped according to the residual principle [8], which consists in performing iterations in order to have satisfy the condition:

$$\left\|\widehat{Y} - CAw^{m+1}\right\|^2_{L_2} \leqslant \|C\|^2_{L_2}\sigma_T^2 \tag{20}$$

Iterations are needed only to eliminate a non-linear contribution. Thus, the total number of iterations is rather small. However, the linear problem has to be solved at each iteration step. A widely used method for IHTP solution is the iterative regularization method [4,10], based on the conjugate gradient algorithm, see [10,11]. For this method the number of iterations required for solving non-linear inverse problems is nearly the same as for linear problems. This is why under normal circumstances the conjugate gradient algorithm is preferable. In this study the most time-consuming part is the recalculation of coefficients u, v, Φ, which requires the solution of N–S equations. Therefore, the iterative process (18), (19) is preferable.

4.2. Numerical solution of the linear IHTP

To compute the solution of the linear IHTP, the Tikhonov's regularization method [12] has been used. For a given m, Eq. (18) is solved by minimizing the following convex quadratic functional

$$J(w) = \left\| f^m - CB^n w\right\|^2_{L_2} + \alpha^2 \|w\|^2_{W_2^2} \tag{21}$$

The unique optimal solution $w^{m+1}(\alpha)$ depends on the regularization parameter α, which has to be chosen from the generalized residual principle

$$\left\| f^m - CB^n w^{m+1}\right\|_{L_2} = \chi \tag{22}$$

$$\chi = \|C\|^2_{L_2}\sigma_T^2\big(1 + \varepsilon(m)\big) \tag{23}$$

where $\varepsilon(m) \to 0$ is a monotonic decreasing function of m.

The unknown function $w(r)$ to be determined is approximated by a piecewise constant function

$$w(r) = \sum_{j=1}^{N_r} w_j \pi_j(r); \qquad \bar{w} = \{w_j,\ j = 1, \ldots, N_r\}$$

where

$$\pi_j(r) = \begin{cases} 1, & \text{if } r \in \left[(r_j + r_{j-1})/2,\ (r_j + r_{j+1})/2\right] \\ 0, & \text{elsewhere} \end{cases}$$

and the measurements $\widehat{Y}_k(x)$ by vectors $\overline{\widehat{Y}}_k(x_i)$: $i = 1,\ N_x$. Consequently, a finite-dimensional form of operator CB^n is a matrix $\overline{B}$ and a finite-dimensional form of the vector-function f^m is a vector $\bar{f}^m$. Then the functional (21) to be minimized can be written in the finite-dimensional form

$$J\left(\bar{w}^{m+1}\right) = \left\|\bar{f}^m - \overline{B}\bar{w}^{m+1}\right\|^2_{L_2} + \alpha^2\left\|F\bar{w}^{m+1}\right\|^2_{L_2} \tag{24}$$

By using a standard singular value decomposition (SVD) of the linear operators, the optimal solution takes the form

$$\bar{w}^{m+1} = F^{-1} V S_\alpha^{-1} U^{\mathrm{T}} \bar{f}^m \tag{25}$$

$$S_\alpha^{-1} = \operatorname{diag}\left\{s_j^{-1} = s_j/\left(s_j^2 + \alpha^2\right)\right\}$$

where the matrixes U, V, S are the SVD factors of $\overline{B}F^{-1}$. These factors have to be recalculated only when the matrix $\overline{B}$ is changed.

The optimal value of the regularization parameter α is given by the solution of the non-linear algebraic equation, which is solved iteratively [9]:

$$\sum_{j=1}^{N_r} g_j^2 \alpha^4 / \left(\alpha^2 + s_j^2\right)^2 + \sum_{j=N_r+1}^{N_x} g_j^2 = \chi$$
$$\bar{g} = U^{\mathrm{T}} \bar{f}^m \tag{26}$$

5. The direct problem solution method

The direct problem is solved at each iteration in order to calculate the right-hand side of Eq. (18). The computational strategy chosen is based on a coupled block-implicit solution approach [3,14]. The numerical solutions of the problem are computed in a cylindrical domain. The new variable was used:

$$r'(x) = r/R(x)$$

It gives

$$f_x = f_x + \beta(x) r' f_{r'}, \qquad f_r = R^{-1}(x) f_{r'}$$
$$\beta(x) = -R_x(x)/R(x)$$

According to these substitutions, the energy equation for the cylindrical domain $(0, L) \times (0, 1)$ can be rewritten in the form

$$\left(uT_x + \left(u\beta(x)r' + vR^{-1}(x)\right)T_{r'}\right) = \frac{1}{Pe}\left[\left(T_x + \beta(x)r'T_{r'}\right)_x + \beta(x)r'\left(T_x + \beta(x)r'T_{r'}\right)_{r'}\right] + \frac{R^{-2}(x)}{Pe}\left[\frac{1}{r'}(r'T_{r'})_{r'}\right] + \frac{Ec}{Re}\Phi \tag{27}$$

The same transformations have been done with Eqs. (1)–(3) and (5), but for simplicity, the details are not be presented here. This coordinate transformation provides a good "physical" mesh that allows to reduce the total number of grid nodes in the radial direction. In addition, the normal derivative at the interface polymer-die will coincides with the radial derivative. This is convenient even if a non-adiabatic condition at the channel wall is considered.

The continuity equation is held in its original form in terms of velocities, but small non-zero elements are placed on the diagonal of the coefficient matrix to eliminate the need for reordering. The momentum and continuity equations are discretized using the control volume approach on a non-uniform staggered grid according to a nine-point stencil and arranged in a block-wise structure

$$\bar{y} = \{y_k\}$$
$$y_{(i-1)N_r+j} = (u_{i,j}, v_{i,j}, p_{i,j}), \quad i = 1, N_x, \ j = 1, N_r \tag{28}$$

The resulting large set of non-linear equations is presented in the form

$$G^n \bar{y} = \bar{z} \tag{29}$$

It is solved iteratively

$$\bar{y}^{m+1} = \bar{y}^m + t\left(G^n\right)^{-1}\left(\bar{z} - G^m \bar{y}^m\right), \quad m > n \tag{30}$$

where the coefficient matrix G^n in Eq. (29) is computed for the approximation of the viscosity and temperature fields at the iteration $n \leqslant m$ and t is an under-relaxation parameter. Like the operator B^n in Eq. (18), the matrix G^n should not be change within iteration loop. The matrix G^n is not inverted: the resolution is performed using a LU-decomposition of G^n. This is the most time-consuming operation: the matrix has the dimension $3N_xN_r$ with a $3N_r + 2$ bandwidth, and the total number of flops required is about $54N_xN_r^3$.

The same approach is used for the temperature field computation. Eq. (27) is discretized on a grid where the temperature control volume coincides with the control volume for u-velocity. The resulting set of non-linear equations is presented as in the form of Eq. (29) and it is solved by using the same iterative process as in Eq. (30). The dimension of the matrix is N_xN_r with a $N_r + 2$ bandwidth. Therefore, the total number of flops required for matrix LU-decomposition is about $2N_xN_r^3$.

An evaluation of the matrix $\overline{B}$ for Eq. (18) requires N_r applications of the temperature field solution procedure, which gives in total the same amount of calculations as a single decomposition of the coefficient matrix G^n.

The accuracy of the direct problem solution is related to the value of χ, cf. Eq. (23). The idea is to stop the iterative solution of the direct problem when the temperature along the measurement lines is not corrected significantly. The following stopping criteria [3] are used:

$$\begin{cases} \left|K^{m+1} - K^m\right| / K^m \leqslant \varepsilon_1 \\ \left\|Y^{m+1} - Y^m\right\|_{L_2}^2 \leqslant \varepsilon_2 \chi \end{cases}$$

where K^m is the kinetic energy of the flow and ε_1, ε_2 are empirical constants.

6. Results and discussion

Numerical simulations of the direct and inverse problem solutions are computed under the following practical injection conditions. The channel geometry is given in Fig. 2. The

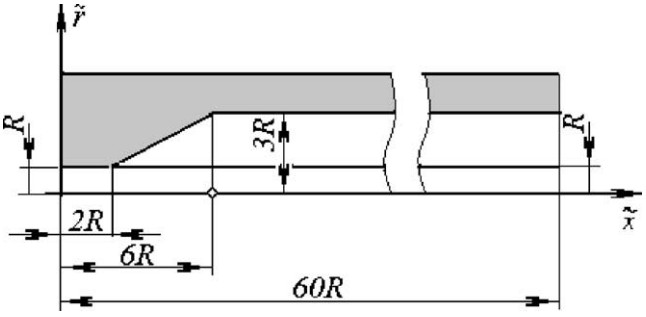

Fig. 2. Channel geometry including an expanded part followed by a straight part.

widely used polymer melt PBT (Valox 420) is chosen, with the following properties:

$\eta_{\text{ref}} = 2950\ \text{kg}\cdot\text{m}^{-1}\cdot\text{s}^{-1}$, $\nu = 0.59$
$\beta = -0.024\ \text{K}^{-1}$, $T_{\text{ref}} = 423\ \text{K}$
$\lambda = 0.25\ \text{W}\cdot\text{m}^{-1}\cdot\text{K}^{-1}$, $\rho = 800\ \text{kg}\cdot\text{m}^{-3}$
$c = 2400\ \text{J}\cdot\text{kg}^{-1}\cdot\text{K}^{-1}$.

Typical values are taken for the channel radius $R = 0.0015\ \text{m}$ and for the reference velocity $u_{\text{ref}} = 0.3\ \text{m}\cdot\text{s}^{-1}$. They lead to the dimensionless parameters values:

$$Re = 1.22 \times 10^{-4}, \qquad Pe = 3456, \qquad Ec = 1.5 \times 10^{-7}$$

The mesh size in the axial and in the radial directions is fixed by the node numbers respectively equal to $N_x = 81$, $N_r = 21$.

An adiabatic condition, $q_w = 0$, is considered and measurement data $\widehat{Y}$ are assumed to be available at each grid node along the channel boundary. How to provide such measurements in practice is a separate issue. Solving a conjugate heat transfer problem by including the die in the spatial domain of the IHTP could be a possible way to overcome this difficulty. For simplicity, this issue is not considered in this study.

The standard deviation of the measurement errors is taken to be $\sigma_T = 0.1$ K and the constants in the stopping criteria, Eq. (31), are chosen equal to $\varepsilon_1 = 0.02$ and $\varepsilon_1 = 0.01$.

Some results of the IHTP solution are presented in Fig. 3, where test inlet temperature functions $w(r)$ are chosen as Gaussian functions of the radial variable:

$$w(r) = 10\exp\left(-7.5(r-a)^2\right)$$

The maximal temperature rise can be easily shifted in the radial direction, by changing the parameter value $a = 0.8$, 0.7, 0.6, 0.5.

Only temperature measurements along the boundary of the channel ($N = 1$) are considered to solve the inverse problem. It can be noted on Fig. 3 that the accuracy of the restoration of $w(r)$ depends on the parameter a. For $a = 0.8$, 0.7, the distance $(1 - a)$, between the location of the maximal temperature rise of the inlet profile and the inlet channel boundary, is small enough and the accuracy of the restoration is quite acceptable, but it drops quickly when the parameter a approaches zero. These results are not surprising, because by taking temperature measurements only at the channel boundary, there is a lack of information from the central part of the flow, and the restoration of the inlet profile is more difficult in the central part than in the part close to the boundary. However in practice, from a thermal analysis point of view, the flow region near the channel boundary is the most interesting. For narrow channels, viscous dissipation, chemical reactions, solidification, and slipping phenomena are commonly generated close to the channel boundary. Therefore, the suggested approach aims to be efficient at least for investigating the thermal effects of such phenomena which occur in this flow region.

In order to illustrate this idea, we carried out a numerical experiment where the inlet temperature profile $w(r)$ to be determined, was chosen as the outlet profile of an upstream polymer flow through a straight channel. This upstream cylindrical channel was chosen with constant radius R and with length $L = 40R$. Such flow conditions are those of an experimental die used for an injection process. The results of the inverse problem solution under this inlet condition are presented in Fig. 4, mark 1. As shown, $w(r)$ given by the continuous curve, is restored almost perfectly. Moreover, several numerical simulations confirmed that the restoration accuracy of $w(r)$ is improved by increasing the accuracy of measurements. It can be noted that the inlet temperature profile corresponding to fully developed thermal conditions was computed with a fixed temperature condition at the wall, then the inlet profile does not satisfy the adiabatic condition

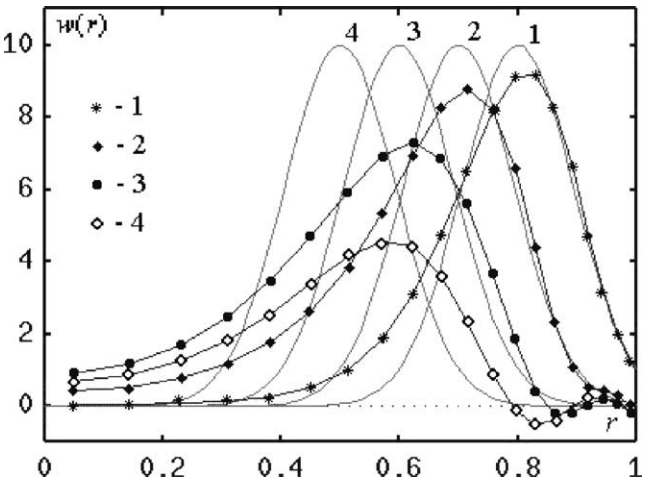

Fig. 3. Four test inlet functions (lines 1–4; no marks) compared with the computed optimal IHTP solutions (1) $a = 0.8$; (2) $a = 0.7$; (3) $a = 0.6$; (4) $a = 0.5$ (4 lines with marks) for an expanded channel and one measurement line ($N = 1$).

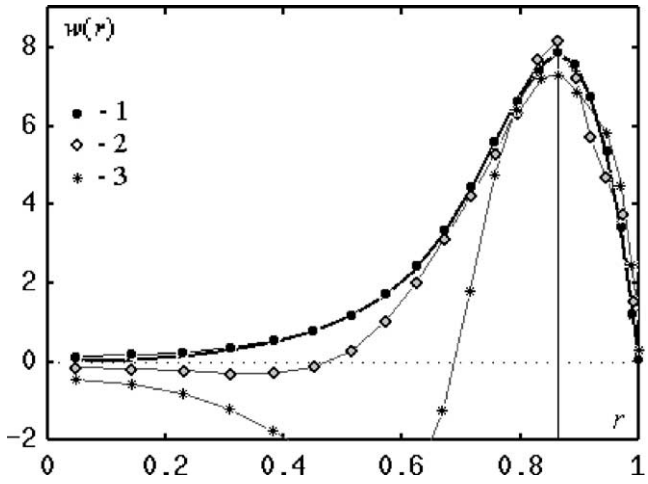

Fig. 4. For one measurement line ($N = 1$), an inlet temperature profile corresponding to fully developed thermal conditions (heavy line, no marks) is compared with: the optimal IHTP solution (curve 1); the IHTP solution after $n = 1$ for an expanded channel (curve 2); the IHTP solution after $n = 1$ for a straight channel (curve 3).

at the wall and the radial temperature gradient is different from zero.

Other results show the influence of the iteration number of the sequential approximation method. Some of the approximated inlet functions $w(r)$ presented in Fig. 4, are obtained at the first iteration ($n = 1$) of Eq. (18), without taking into account the coupling between the temperature and the velocity fields. One result (mark 2) is obtained for the expanded channel, while another result (mark 3) is for a straight channel. The maximal temperature rise for the straight channel is almost ten times greater than that for the expanded channel; this is because it causes more non-linear effects, which have to betaken into account by increasing the number of iterations.

The results presented in Fig. 5 illustrate the advantage in taking additional measurements, $N = 2$, at the centerline $R_2(x) = 0$ ($x > 6R$). The restored inlet profile $w(r)$ for this case, is the dotted curve 2. The continuous curve is the same curve 3 as in Fig. 3. As expected, when additional data are used for solving the IHTP, the total accuracy of the restored inlet profile $w(r)$ is improved, more importantly so in the region that is close to the centerline. Restored values near the channel boundary wall are almost not affected. Therefore, the location of the measurement lines has to be chosen according to the flow region of interest. In practice, these additional data from the central region of the flow could be collected by installing a sensor like a torpedo in the channel. Such an intrusive body within the polymer flow will distort the velocity and the temperature fields. For such a situation, a conjugate heat transfer model including both the polymer and the torpedo should be considered in the IHTP statement.

The results presented in Fig. 5 also illustrate the influence of the channel geometry. The restored inlet profile $w(r)$, given by the dotted curve 3, corresponds to the IHTP solution obtained with the straight channel of radius R, using only the boundary channel data ($N = 1$). Note that the restoration accuracy is worse than for the expanded channel. This result can be explained by the fact that within the expanded region of the channel, there is a convective heat transfer from the central region of the flow toward the channel boundary, in addition to heat transfer provided by conduction in the polymer melt. Consequently, it has been observed that the convergence history of the iterative process for restoring the above inlet profiles $w(r)$ also depends on the channel geometry. For the expanded channel the total number of iterations required to satisfy the criterion (20) was less than four. The matrix $\overline{B}^n$ in Eq. (18) and its SVD-decomposition was recomputed once at $m = 2$. For the straight channel the number of iterations required was between five and eight, and the matrix $\overline{B}^n$ was recalculated up to three times. No additional LU-decompositions of the coefficient matrix G^n in Eq. (30) was required. The total number of simple iterations in the iterative process (30) used was up to ten, both for the flow problem and for the energy equation.

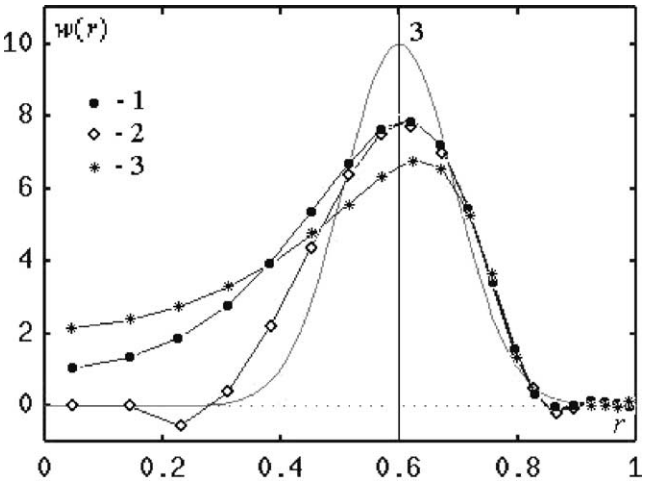

Fig. 5. A Gaussian inlet function ($a = 0.6$; line without marks) is compared with computed IHTP solutions: (curve 1) with the expanded channel and $N = 1$; (curve 2) with the expanded channel and $N = 2$, additional measurements at centerline ($x > 6R$); (curve 3) with the straight channel and $N = 1$.

7. Conclusion

A new approach based on the numerical solution of an IHTP has been presented to investigate the thermal behavior of a polymer melt flowing through narrow channels. This approach could provide more accurate heat transfer modeling, especially in the radial direction within cylindrical channels, than methods based only on the bulk temperature analysis of the melt. The main goal of the paper was to demonstrate the feasibility of this method.

Due to the high temperature dependence of the polymer melt viscosity, the inverse heat transfer problem cannot be solved without considering the coupling between the velocity and the temperature fields. It requires repeated solutions of the full Navier–Stokes equations at each step of the iterative procedure. In order to reduce the number of calls to the Navier–Stokes solver, the sequential approximation method regularized in the Tikhonov sense, has been developed and found to be quite efficient. A strongly coupled block-implicit approach was used for solving the fluid flow equations, together with a direct LU-decomposition for solving algebraic equations. This approach exploits the idea that an initial approximation of the velocity field, calculated for a reference temperature, is already close to the solution. However, it cannot be recommended as a fast solver in general: its application is restricted to steady state and two-dimensional cases.

The presented simulation results illustrate how the radial inlet temperature profile can be restored with a good accuracy in the annulus region $0.7 < r < 1$, located close to the inlet channel boundary when the measured restoring data is obtained only at the walls. Therefore, the method could be used for investigating heat transfer near the channel wall. The effect of the channel geometry has also been illustrated. The use of an expanded channel as a separate experimen-

tal device would provide more instrumental freedom than a straight channel.

Acknowledgements

The authors would like to thank “Le Conseil Régional des Pays de la Loire” for the financial support provided to this work and the reviewers for their helpful suggestions for improvement of the manuscript.

References

[1] P. Lin, Y. Yaluria, Conjugate transport in polymer melt flow through extrusion dies, Polymer Engrg. Sci. 37 (1997) 1582–1595.
[2] P. Lin, Y. Yaluria, Heat transfer and solidification of polymer melt flow in a channel, Polymer Engrg. Sci. 37 (1997) 1247–1258.
[3] G.C. Vradis, K.J. Hammad, Strongly coupled block-implicit solution technique for non-Newtonian convective heat transfer problems, Numer. Heat Transfer B 33 (1998) 79–97.
[4] O.M. Alifanov, Inverse Heat Transfer Problems, Springer-Verlag, Berlin, 1994.
[5] Ch.-H. Huang, W.-Ch. Chen, A three-dimensional inverse forced convection problem in estimating surface heat fluxes by conjugate gradient method, Internat. J. Heat Mass Transfer 43 (2000) 3171–3181.
[6] M. Prud’homme, T.H. Nguyen, A numerical solution for the inverse natural convection problem, Numer. Heat Transfer A 32 (1997) 169–185.
[7] J.F. Agassant, P. Avenas, J.Ph. Sergent, P.J. Carreau, Polymer Processing, Hanser Publishers, 1991.
[8] O.M. Alifanov, I.Yu. Gejadze, A method for on-line identification of thermal loads, J. Engrg. Phys. 71 (1998) 30–40.
[9] I.Yu. Gejadze, On-line methods for heat transfer identification in flight vehicle structures, Ph.D. Thesis, Moscov Aviation Institute, Russia, 1998.
[10] O.M. Alifanov, E.A. Artyukhin, S.V. Rumyantsev, Extreme Methods of Solving Ill-Posed Problems and Their Application to Inverse Heat Transfer Problems, Begell House, New York, 1995.
[11] Y. Jarny, M.N. Ozisik, J.P. Bardon, A general optimization method using adjoint equation for solving multidimensional inverse heat conduction, Internat. J. Heat Mass Transfer 34 (1991) 2911–2919.
[12] A.N. Tikhonov, V.Ya. Arsenin, Solving of Ill-Posed Problems, Winston and Sons, Washington, DC, 1977.
[13] M.M. Lavrent’ev, V.G. Romanov, S.P. Shishatskiĭ, Ill-Posed Problems of Mathematical Physics and Analysis, American Mathematical Society, Providence, RI, 1986.
[14] M.E. Braaten, Development and evaluation of iterative and direct methods for the solution of the equations governing recirculating flows, Ph.D. Thesis, University of Minnesota, 1985.